# A Chemical Screen Identifies Class A G-Protein Coupled Receptors As Regulators of Cilia

Prachee Avasthi,[†] Aaron Marley,[‡] Henry Lin,[§] Elisabet Gregori-Puigjane,[§] Brian K. Shoichet,[§] Mark von Zastrow,[‡] and Wallace F. Marshall*,[†]

Departments of [†]Biochemistry & Biophysics, [‡]Psychiatry, and [§]Pharmaceutical Chemistry, University of California, San Francisco, California 94158, United States

S *Supporting Information*

ABSTRACT: Normal cilia length and motility are critical for proper cellular function. Prior studies of the regulation of ciliary structure and length have primarily focused on the intraflagellar transport machinery and motor proteins required for ciliary assembly and disassembly. However, several mutants with abnormal length flagella highlight the importance of signaling proteins as well. In this study, an unbiased chemical screen was performed to uncover signaling pathways that are critical for ciliogenesis and length regulation using flagella of the green alga *Chlamydomonas reinhardtii* as a model. The annotated Sigma LOPAC1280 chemical library was screened for effects on flagellar length, motility, and severing as well as cell viability. Assay data were clustered to identify pathways regulating flagella. The most frequent target found to be involved in flagellar length regulation was the family of dopamine binding G-protein coupled receptors (GPCRs). In mammalian cells, cilium length could indeed be altered with expression of the dopamine D1 receptor. Our screen thus reveals signaling pathways that are potentially critical for ciliary formation, resorption, and length maintenance, which represent candidate targets for therapeutic intervention of disorders involving ciliary malformation and malfunction.
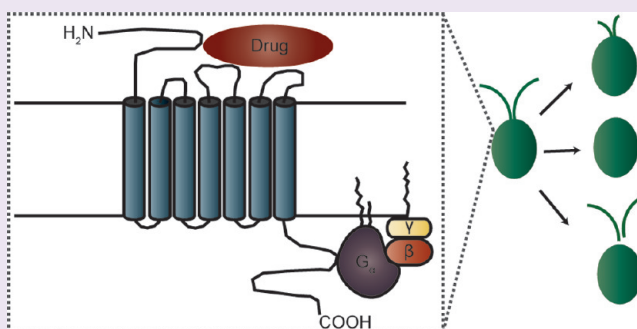
Cilia and flagella are microtubule-based organelles that protrude from the cell surface. Nine microtubule doublets form the ciliary axoneme, which is ensheathed by plasma membrane. The doublets extend from microtubule triplets of the basal body that anchors it. A kinesin-based trafficking system called intraflagellar transport (IFT) is required for assembly and maintenance of cilia.[1−5] Cilia are conserved organelles present on virtually every cell of the human body and are responsible for sensing the environment and driving fluid flow.

Cilia length is tissue-dependent. Abnormal length often accompanies a variety of pathological conditions including Meckel Syndrome, tuberous sclerosis, nephronophthisis, Bardet Biedl Syndrome, and others,[6−13] suggesting that proper length may be important for normal physiological function. However, the mechanisms that regulate ciliary length remain unclear.

Genetic studies in the unicellular green alga *Chlamydomonas reinhardtii* have demonstrated the existence of cilia length regulating pathways. *Chlamydomonas* flagella are virtually identical to cilia of vertebrate cells and provide an excellent model to study ciliary/flagellar length control because *Chlamydomonas* is a single-celled organism amenable to biochemistry and yeast-like forward genetics. Mutations in three genes, SHF1, SHF2, and SHF3, result in short flagella,[14] and mutations in four genes, LF1, LF2, LF3, and LF4, result in long flagella.[15−19] *LF2* encodes a CDK-related kinase,[19] and

LF4 encodes a MAP kinase.[17] The fact that kinase mutations can produce long flagella demonstrates the importance of signaling in length control, but study of these mutants has yet to elucidate the larger pathway of flagellar length regulation.

An alternative to the genetic approach is chemical biology using small molecule modulators of signaling pathways. Previously, several small molecules have been found to modulate cilia length in vertebrate cells. For example, knockdown of a phosphatase inhibitor protein required for primary cilium formation is rescued by a histone deacetylase inhibitor and a protein phosphatase 1 inhibitor.[20] In IMCD3, MEK, and BME cells, molecules blocking calcium entry or release from intracellular stores as well as molecules increasing cAMP cause cilia to elongate.[21] Pharmacological studies in vertebrate cells have relied on a handful of pathway-specific compounds, and no systematic unbiased chemical screens have been reported.

Chlamydomonas, in addition to its advantages for genetics and biochemistry, is also amenable to small molecule studies. Although the *Chlamydomonas* cell body is surrounded by a cell wall, the flagella are entirely exposed to the surrounding growth media. Efficacy of small molecules in changing *Chlamydomonas*

flagellar length has previously been demonstrated. For example, IBMX,[22] colchicine, cytochalasin D,[23] calcium-calmodulin blockers, and Na^+, K^+, EGTA can all induce shortening.[24] Ciliabrevin, a compound identified by a small molecule screen in *Chlamydomonas*, reduces intraflagellar transport and induces shortening[25] However, that screen was conducted with a non-annotated library of diverse compounds and the direct target of ciliabrevin remains unknown. Lengthening is induced in the paralyzed *pf18* mutant by La^{3+} and Cd^{2+} [26] and in wild-type cells by LiCl.[27]

To identify novel pathways involved in flagellar length control in *Chlamydomonas*, we employed an unbiased cell-based chemical screening strategy using an annotated library of small molecules. Clustering of our results identified class A GPCR-dependent pathways as major regulators of flagellar length and motility. These same pathways have recently been gaining attention with respect to their localization to mammalian cilia, and we have shown here that expression of a dopamine receptor subtype can have lengthening effects on cilia in mouse fibroblasts. The cilia-specific function of these receptors in mammalian systems as well as in *Chlamydomonas* has heretofore been largely unknown.

■ RESULTS AND DISCUSSION

Screen for Small Molecule Flagellar Modulators in *Chlamydomonas*. To identify novel pathways modulating flagellar length in *Chlamydomonas*, all 1280 small molecules in the Library of Pharmacologically Active Compounds (LOPAC) (Sigma) were incubated with wild-type CC-125 cells at a final concentration of 100 μM for 2 h. Concentration used for the length screen was empirically determined on the basis of the percentage of compounds found to be active using a subset of the library. The Sigma LOPAC1280 database is a library of well-characterized small molecules annotated to their known targets in mammalian systems. The distribution of these molecular target annotations is shown in Supplementary Figure 1. Each compound was tested for an effect on length by direct microscopy-based measurements. Because of the large number of compounds, a small N of 10 cells per well was chosen for flagellar measurement. This was confirmed to be sufficient to identify true changes in flagellar length based on experiments with known length-altering compounds and mutants, (Supplementary Figure 2). Cells were imaged as described in Methods (Figure 1a), and flagellar length was measured using image analysis software.

Compounds were added to cells at a final concentration of 1% DMSO. Since DMSO concentrations above 1% can affect the length of *Chlamydomonas* flagella,[28] a 1% DMSO-only control was included in each assay plate for comparison to drug-treated cells. Of the compounds, 11.5% caused flagella to be shortened compared to the within-plate DMSO-only controls (Figure 1a middle, Supplementary Table 2). This rather high hit rate is expected given that the LOPAC library contains only compounds with known biological activity. Shortening factors for each compound were calculated as described in Methods and plotted in Figure 1b. The shortening factor for each compound is given in Supplementary Table 1. Several compounds caused a small but statistically significant increase in mean flagellar length compared to controls, but the lengths were still in the wild-type range. Unlike inhibition of GSK3B with LiCl, which significantly increases flagellar length,[27,29] several other GSK3B inhibitors in the LOPAC library did not lengthen flagella. This could be due to the usage
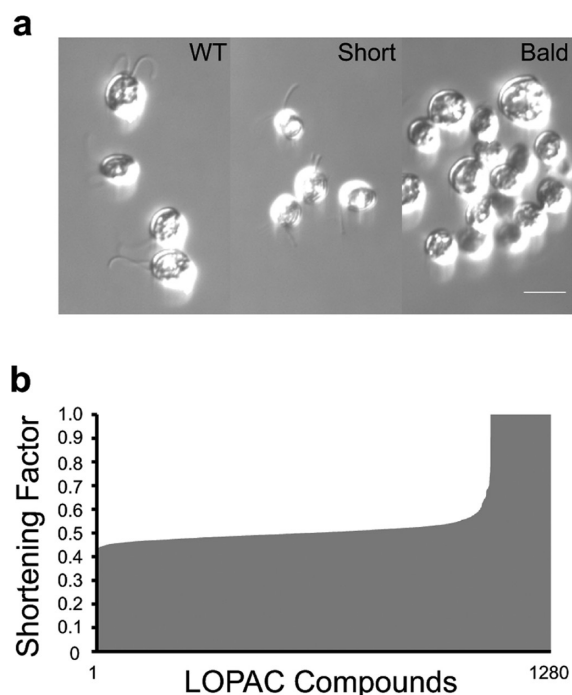

Figure 1. Cell-based small molecule screen in *Chlamydomonas* cells. (a) DIC images of untreated wild-type *Chlamydomonas* cells (left), cells with shortened flagella (center), and cells that lost flagella during drug incubation (right). Scale bar 10 μm. (b) Shortening factors of all LOPAC1280 compounds in ascending order. Maximum shortening factor of 1 corresponds to complete loss of flagella and a shortening factor of 0.5 corresponds to no change in flagellar length.

of a single drug concentration (100 μM) for the screen that is 250-fold lower than the concentration of LiCl known to increase length (25 mM). A similar explanation may account for the lack of observable phenotype when applying CDK-related kinase inhibitors, as mutants of the CDK-related kinase, LF2, have long or short flagella depending on the mutation. Alternatively, the CDK inhibitors known to bind human targets in the LOPAC library may not bind the *Chlamydomonas* LF2p protein. Of the compounds, 10.8% caused bald, flagella-less cells (Figure 1a right, Supplementary Table 3). The largest number of compounds that shortened flagella were known in LOPAC to target selectively a single protein family of dopamine receptors, metabotropic G-protein coupled receptors (GPCRs) that serve critical functions in the brain, heart, and kidney.

Counter-Screen for Cytotoxic Compounds. To eliminate toxic compounds from further consideration, a viability counter-screen was performed to identify the compounds that caused cells to fail to divide following the 2-h drug incubation period. Treated cells diluted in fresh medium were checked for growth after 5 days (Figure 2a). Of the compounds, 3.9% were identified as cytotoxic (Supplementary Table 4).

Identifying Compounds That Induce Flagellar Severing. Under certain environmental conditions, a microtubule severing pathway known as flagellar autotomy or deflagellation is activated that results in loss of flagella rather than resorption. Compounds triggering deflagellation were identified by microscopic visualization of detached severed flagella in the surrounding medium (Figure 2b, arrows, Supplementary Table 5). Of the 126 compounds activating deflagellation, 17% were annotated to target mammalian ion channels in the
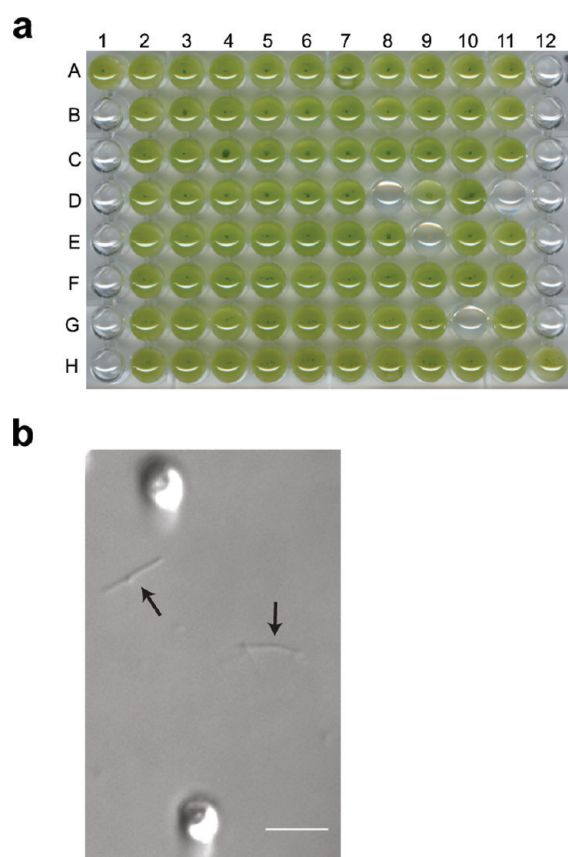
Figure 2. Viability and deflagellation assays. (a) Cells that could not tolerate drug incubation did not divide when diluted and grown in fresh drug-free medium. Cells that survived drug treatment gave visibly green cultures. (b) Cells were considered to activate the deflagellation pathway if severed flagella (black arrows) were visible in the medium during microscopic visualization or in DIC images. Scale bar is 10 μm.

LOPAC database, many of which affected calcium transport. This is consistent with previous reports that alterations in calcium trigger deflagellation in *Chlamydomonas*.[30] Compounds targeting mammalian dopamine and serotonin monoamine GPCRs were also frequent among those that induced deflagellation. Since low pH induces autotomy, we tested three compounds most likely to lower pH based on their pK_a, but in all cases the pH remained approximately 7.5 when added at assay concentrations.

Alternative Motility-Based Screen. The screen reported above was based on direct microscopic measurements. We have developed an alternative assay more suitable to high-throughput screening, exploiting the fact that *Chlamydomonas* cells require normal-length flagella for effective swimming. Motility defects were identified by visualizing cells that pooled at the bottom of U-bottom wells in a 96-well plate rather than swimming throughout the well (Figure 3a). Standard deviations of the image intensities within each imaged well were normalized by the standard deviation of DMSO-only treated cell wells. The ratio of standard deviations was called the pooling factor, P, as illustrated in Figure 3b. This assay was used to rescreen the LOPAC library. Outcomes fell into four qualitatively distinct categories: no pooling, slight pooling, intermediate pooling, and strong pooling. In order to determine which pooling factors corresponded to which category, a
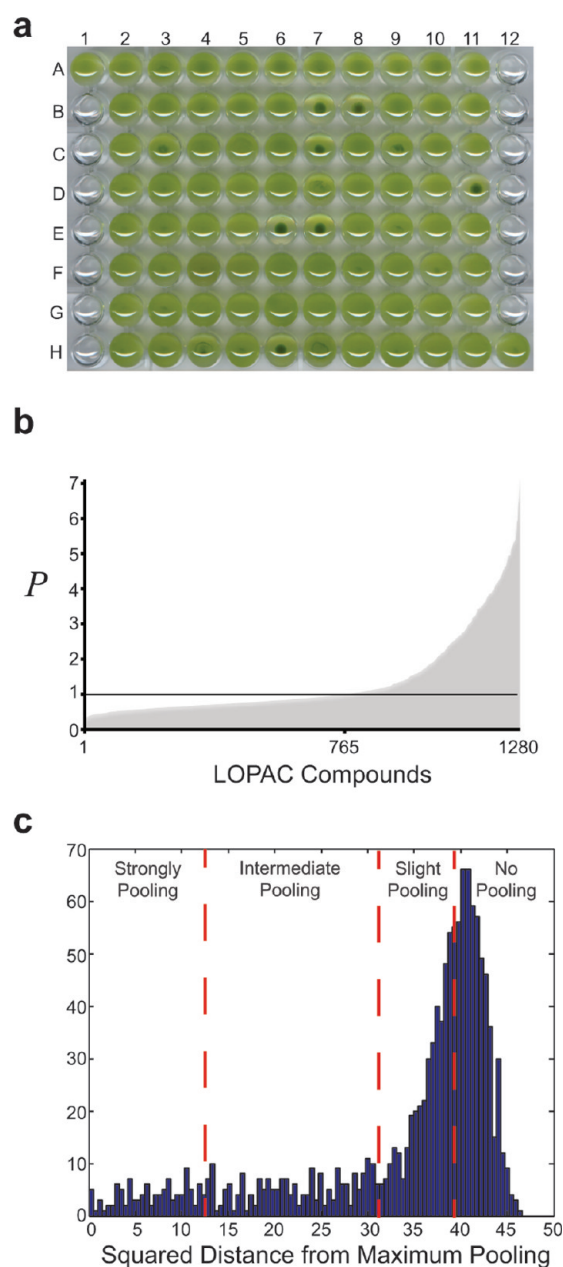

Figure 3. Motility assay. (a) Poorly swimming cells accumulate in U-bottom wells, forming a concentrated dark green pellet at the center. Cells that swim well create a homogeneous distribution. (b) The standardized pooling factors are plotted in ascending order. Cells with the same motility as controls have a pooling factor of 1. (c) Histogram of the difference from maximum pooling factor. Cutoffs are shown between unpooled, slightly pooled, pooled, and strongly pooled cells (vertical red dashed lines). Higher values (greatest distance from maximally pooled control) correspond to less pooled cells.

histogram (Figure 3c) was generated of the following normalized pooling score:

$$(P_{max} - P_{current})^2$$

where P_{max} is the pooling factor of the maximally pooled well and $P_{current}$ is the pooling factor of the well in question . Gaussian mixture modeling identified the means and variances of each of the four distributions. Cutoffs for the four qualitative pooling categories were determined by calculating one standard

deviation outside distribution means and using the weighted averages between them (Figure 3c, red dashed lines).

Comparison of the Two Screens. Flagellar lengths (as judged by direct measurement in the first screen) and motility (as judged by in-well standard deviations in the second screen) were correlated with an R^2 value of 0.50, suggesting that the two screens give related but not redundant results. Despite the significance of this correlation ($p \ll 0.01$), several compounds are outliers. These outliers include compounds causing no change in flagellar length but significant pooling (potentially cells with paralyzed flagella) as well as causing a significant shortening of flagella but no pooling (potentially compounds that affect cell viability or buoyancy).

In considering whether the motility assay can be used to detect flagellar length changes, 10 compounds were false positives (pooling phenotype but not length alteration), and 10 that were not cytotoxic were false negatives (abnormal length but no pooling phenotype). Thus the false positive and false negative rates for the motility screen are approximately 1%. The pooling-based motility assay should thus be useful as a primary screen to identify compounds with a potential effect on length.

Hierarchical Clustering Identifies Potential Signaling Pathways Regulating Flagellar Length Changes. The various assays performed on the 1280 LOPAC compounds include direct flagellar length measurement, motility assay, viability assay, and deflagellation assay. These data sets were combined to perform average linkage clustering (see Methods). This method identified 50 clusters representing distinct phenotypic combinations of all the assays performed (Figure 4). Compounds that were nontoxic and exhibited one or more phenotypic effects are shown in Supplementary Table 6.

One particular cluster included compounds that increase pooling without changing flagellar lengths. Since the pooling assay is designed to score cell swimming, one would expect that these compounds might cause a paralyzed flagella phenotype. Indeed, many compounds in this cluster are known modulators of ciliary beat frequency.[31−33] These include compounds

annotated as targeting dopamine, opioid, and adrenergic receptors. High speed imaging confirmed that compounds within this cluster can modulate flagellar motility (Figure 5).
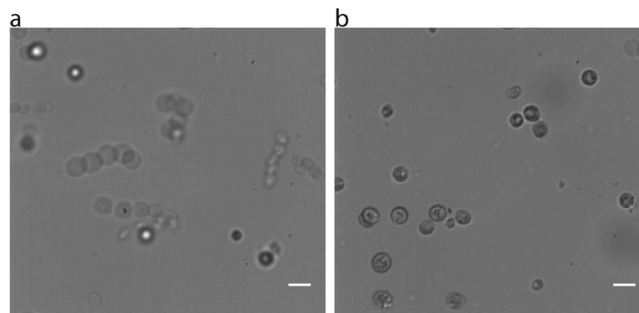
Figure 5. Overlayed still frames of live *Chlamydomonas* cells with and without paralysis-inducing compounds. Overlayed images are 150 frames apart. (a) DMSO-treated control cells swim normally, as seen from the separation between successive cell images. (b) Cells treated with (+)-bromocriptine methane-sulfonate, a dopamine D2 receptor agonist, are virtually immotile. Only one motile cell can be seen in the top right corner. Scale bars 10 μm.

Clustering also grouped compounds that caused cells to lose flagella entirely but without any evidence of severed flagella in the media. These compounds presumably cause flagella to resorb, returning their components to the cell body instead of shedding the flagella into the media. This resorption of cilia and flagella is seen in most cell types prior to mitosis, but the mechanism of resorption and the signals that trigger it remain unclear. Interestingly, of the 30 compounds that cause this phenotype, seven target some class of opioid receptor, the majority of which are κ opioid receptor agonists (Figure 6). We note that in some cases resorbtion may simply be an extreme of the shortening phenotype. We tested four compounds causing flagellar resorbtion without severing and targeting κ opioid receptors based on LOPAC annotations, and all four compounds gave dose-dependent shortening of flagella when applied at lower concentrations (data not shown).

Of the 103 compounds that cause deflagellation in the majority of cells, significant target annotations include ion channels (14.6%); monoamine reuptake mechanisms largely for serotonin (8.7%); and kinases (8.7%). By far the most frequent targets are the class A GPCRs (48.5%). Two clusters within this group, characterized by intermediate and significant levels of pooling, respectively, consist of compounds targeting distinct subclasses of GPCRs (Figure 6): 73% of dopamine receptor targeting compounds in the flagella-less, severing-inducing group cause intermediate pooling in the motility assay, while 88% of histamine receptor targeting compounds and 69% of compounds targeting serotonin receptors in this group cause strong pooling in the motility assay.

The clustering method described here is only one of many possible methods that can be used to facilitate separation unique phenotypes. The metric used to create the distance matrix is imperfect in its ability to identify compounds that cause flagella to be statistically shorter than wild-type length. In a few cases, larger clusters contain a mixture of compounds with different effects on length. However, the rough clustering is useful for primary phenotypic separation so patterns can then be easily identified manually.

GPCRs in *Chlamydomonas*. Since the LOPAC library is annotated with mammalian targets, we have to base our
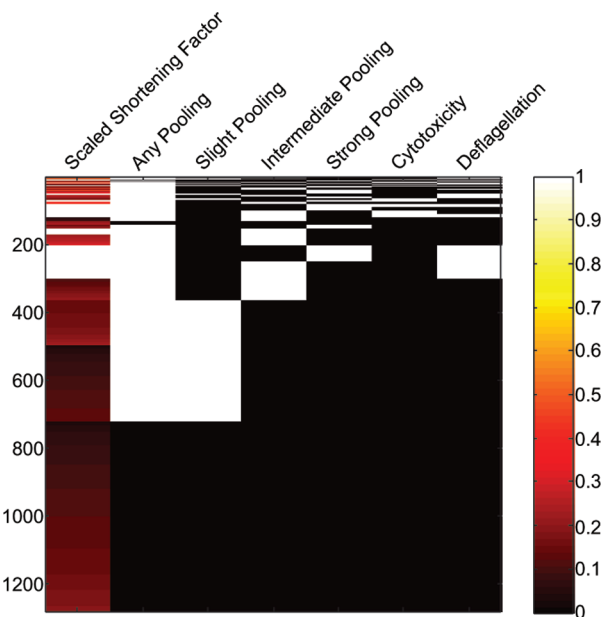

Figure 4. Hierarchical clustering of length, viability, deflagellation, and motility data. Colormap of cumulative assay data shows input values and is arranged by cluster (50 total clusters).
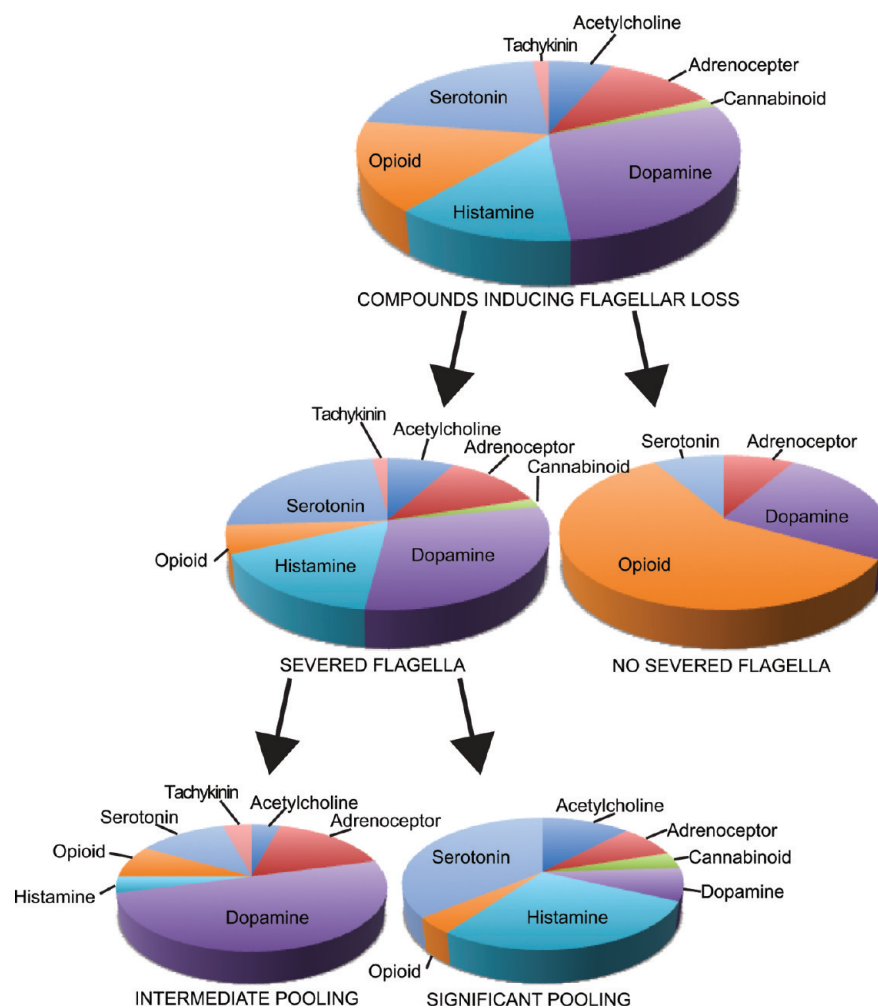
Figure 6. Segregation of GPCR subtypes with length and motility phenotypes. Compounds causing flagellar resorption with no evidence of severed flagella target largely opioid receptors (middle tier, right pie). For the deflagellation-inducing group, the cluster that represents cells with intermediate pooling contains predominantly dopamine receptor targeting compounds (bottom tier, left pie), while the cluster representing cells with significant pooling contains predominantly histamine and serotonin targeting compounds (bottom tier, right pie).

pathway inference on the assumption that similar targets exist in *Chlamydomonas*. Dopamine receptors are found throughout eukaryotes but with high sequence divergence outside of metazoa. Therefore, simple sequence homology searching cannot be used to test whether particular dopamine receptor classes exist in Chlamydomonas. Instead, we took a chemo-informatic approach by searching among our candidate compounds for chemically diverse structures that are known to target the same receptors in mammalian cells and which in our assays resulted in a common phenotype in *Chlamydomonas*. While it is accepted that many small molecules show promiscuity among different protein targets in a cell, the most chemically different two compounds are, the less likely they are to share these off-targets. Having chemically diverse compounds with the same phenotype suggests that their shared targets mediate the phenotype. Two such examples can be found in Figure 7. Four compounds with quantifiably different chemical structure were found that caused flagellar severing and strong pooling in the motility assay (Figure 7a). As is the case with many small molecules, each are known in the literature to bind several off-targets but bind only a single common on-target, the $\alpha 1$ adrenergic receptor, suggesting that an analogous target is associated with the observed phenotype. Similarly, four

structurally diverse compounds that target the dopamine D1 and D2 receptors cause flagellar shortening (Figure 7b).

The shared outcomes of applying these compounds suggest that the reported phenotypes are not off-target effects.

Dopamine Receptor Subtype Overexpression Alters Cilium Length in NIH3T3 Cells. Previous studies have suggested the importance of the role of GPCRs in mammalian ciliary functions. In mice, GPCRs are known to transport to cilia using targeting sequences and utilize ciliary Bardet−Biedl syndrome proteins to modulate their localization.[34−38] Mono-amine GPCRs are also found on most mammalian sperm and regulate their flagellar motility.[39] Recently, activation of dopamine D5 receptor, which localizes to cilia in vascular endothelial cells, was shown to increase cilium length.[40]

In light of our results detailed above, we directly tested whether dopamine D1 receptor signaling could affect length in mammalian cilia. NIH3T3 cells were transfected with a FLAG tagged dopamine D1 receptor construct. The D1 receptor localized to cilia (Figure 8g,j), and expressing cells had significantly longer cilia than untransfected controls (Figure 8k). Transfection of a non-cilium-localized receptor, the transferrin receptor, did not have cilium length altering effects (Figure 8e,k). Basal activity of the receptor is evidently
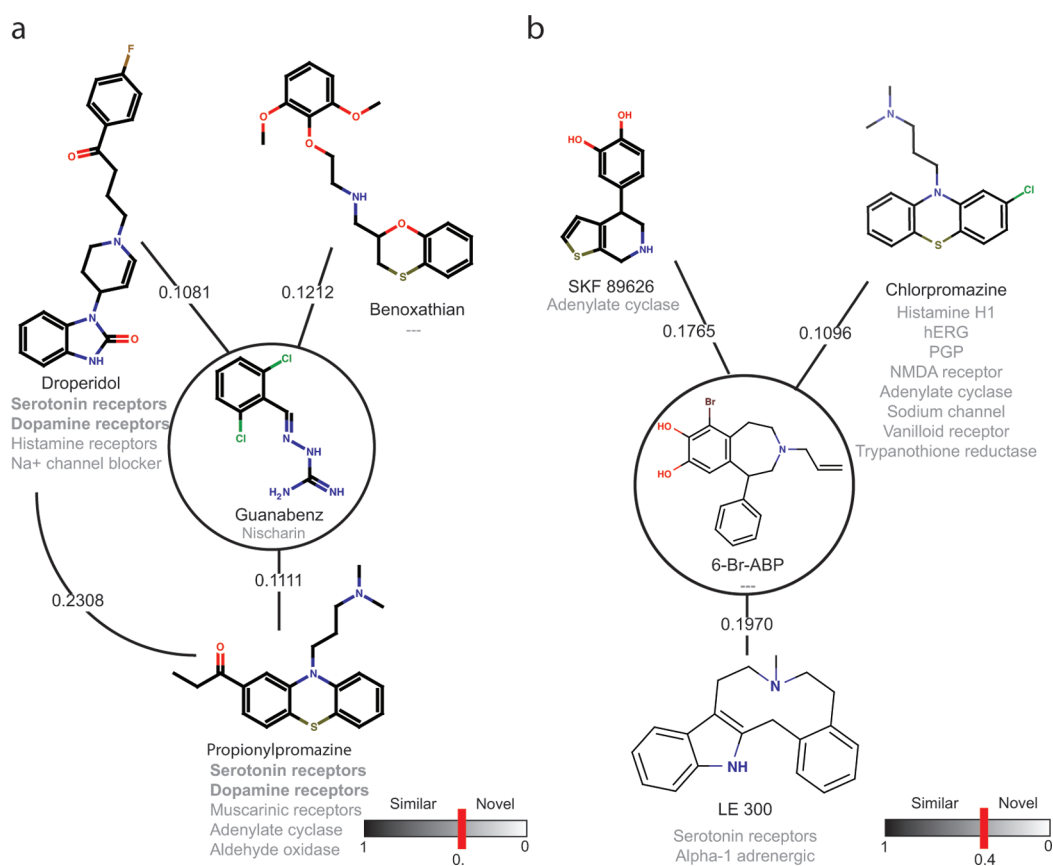
Figure 7. Chemical diversity of common-target compounds causing identical phenotypes. (a) Schematic representation of four α-adrenergic ligands, guanabenz, droperidol, benoxathian, and propionylpromazine, with high chemical diversity. The Tanimoto coefficients among guanabenz and the other three compounds are shown, together with the value for this coefficient between droperidol and propionylpromazine. Their respective off-targets are displayed in gray, showing that although droperidol and propionylpromazine share the serotonin and dopamine receptors, the only target these four diverse compounds share is the α-adrenergic receptor. All four compounds cause flagellar severing and strong pooling. (b) Schematic representation of three dopaminergic ligands, diphenhydramine, 6-bromo-ABP, and LE300, with high chemical diversity. Tanimoto coefficients between diphenhydramine and the other two compounds are shown. Their respective off-targets are displayed in gray, showing that the only target these three diverse compounds share are dopamine receptors. All of these compounds cause flagellar shortening.

sufficient to alter cilium length. The proteins that bind the dopamine receptor targeting compounds in *Chlamydomonas* may have functions different than those of their mammalian counterparts, possibly explaining the different cilium length altering phenotype seen in flagella (see "GPCRs in *Chlamydomonas*" above). Alternatively, basal signaling may produce different results than activation or inhibition achieved using the compounds in the chemical library.

Overview. This study utilized the LOPAC 1280 small molecule library to identify novel pathways that regulate flagellar length. Excluding the 50 compounds that were cytotoxic to *Chlamydomonas* cells, 142 compounds out of the remaining 1230 caused a statistically significant ($p < 0.05$) shortening of flagella, 133 resulted in flagella-less cells, and 126 activated the deflagellation pathway. The largest class of compounds that were active in altering flagellar length in any of these three ways targeted the G-protein coupled receptors that endogenously bind biogenic amines, including acetylcholine, serotonin, histamine, and the catecholamines (epinepherine, norepinepherine, and dopamine). While a large percentage of the LOPAC library includes GPCR-interacting compounds, the proportion of flagellar phenotype inducing compounds that target GPCRs is significantly greater. Of the compounds that cause flagellar shortening, 33% were classified as amine-binding GPCRs, while the fraction of the entire library targeting these

receptors was only 27%. This represents a highly significant enrichment for this class of compounds relative to the frequency in the whole library ($P < 1 \times 10^{-6}$ based on binomial statistics), suggesting that such compounds show a highly significant non-random tendency to induce flagellar shortening. Length-regulating effects of dopamine receptor activation were confirmed using expression of D1 receptors in NIH3T3 cells. Basal activity of the expressed D1 caused an increase in cilium length compared to untransfected and non-ciliary transferrin receptor controls.

Of the flagellar loss inducing compounds (resulting in bald cells irrespective of activation of flagellar autotomy), 37% also target biogenic amine binding GPCRs. The similarity in classes that are targeted frequently regardless of phenotype suggests that shortening and loss of flagella are mechanistically coupled, as suggested by prior genetic studies.[41]

Significance. This work presents the first systematic probing of cilia, an important organelle, using an annotated chemical library. In addition to the raw flagellar length measurement data for each compound, which will be a valuable community resource, this study highlights the utility of combining multiple small molecule screening assays to identify novel pathways critical for normal cellular and organellar function and has allowed us to draw a significant new biological conclusion that G-protein coupled receptor (GPCR) mediated
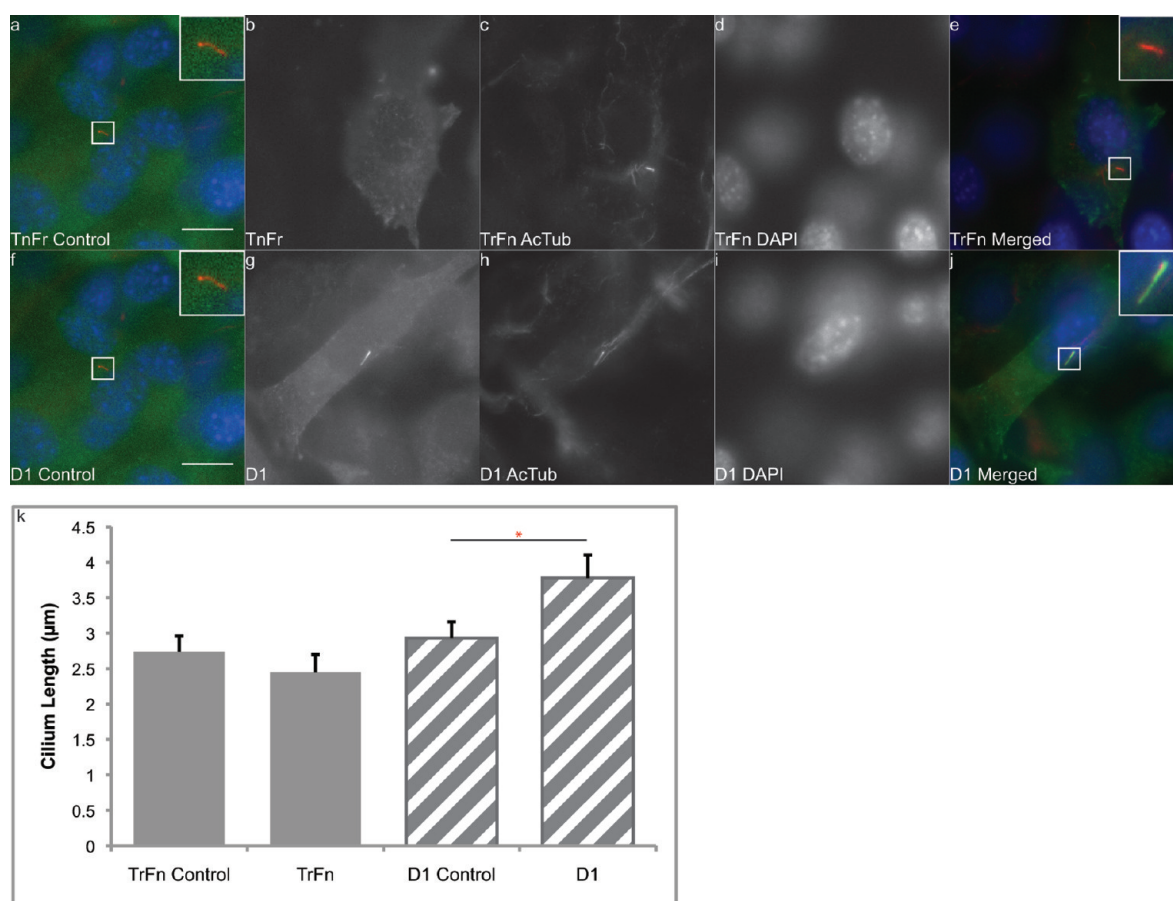
Figure 8. Dopamine receptor expression increases cilium length in fibroblasts. (a−e) Flag-tagged transferrin receptor expressed as a control. (f−j) Flag-tagged dopamine D1 receptor expression. (a, f) Untransfected control cells. Receptor in green, acetylated tubulin labeling cilia in red, DAPI labeling nuclei in blue. Scale bars are 10 μm. (b) Transferrin receptors are not localized to cilia. (g) D1 receptors are localized to cilia. (c, h) Acetylated tubulin labels cilia brightly. (d, i) DAPI labeling of cell nuclei. (e, j) Merged images show increased cilium length with D1 receptor expression compared to transferrin receptor controls. (k) Quantification of cilium length showing significant increase in cilium length with D1 receptor expression compared to untransfected controls on the same coverslip ($N = 28$ for D1 receptor expression and for corresponding untransfected controls, $p < 0.0001$). The transferrin receptor control showed a slight but statistically insignificant reduction in length compared to untransfected controls ($N = 31$ for transferrin expression, $N = 29$ for corresponding untransfected control, $p = 0.0748$). Error bars are 95% confidence intervals.

signaling may be involved in multiple aspects of ciliary regulation. Sporadic prior evidence exists in the literature for the presence of individual GPCRs in the ciliary compartment and their role in ciliary motility and maintenance. However, this work identifies entire GPCR families within Class A that are coupled to a phenotypic signature. Because GPCR-targeting compounds and related modulators of identified pathways have well-understood pharmacological properties, we suggest that they may show high therapeutic potential for treating the growing list of cilia related disorders.

■ METHODS

Drug Treatment, Flagellar Length Measurements, and Deflagellation Assay. CC-125 cells were grown in liquid Tris-acetate-phosphate (TAP) medium from TAP-agar plates for 24 h in continuous light on a roller drum. Next, 100 μL of cells and 1 μL of 10 mM compounds resuspended in 100% DMSO from the LOPAC1280 library (Sigma) were added to U-bottom 96-well plates. Drug-treated cells were incubated on the benchtop without agitation for 2 h and fixed by adding 100 μL of 2% glutaraldehyde. Fixed cells were imaged by DIC microscopy at 40×, and flagellar lengths were measured by line segment tracing and spline fitting in ImageJ. Compounds for which severed flagella were seen by direct microscopic inspection or later seen in saved images were noted.

Degree of flagellar shortening was reported as a shortening factor, defined as follows:

$$S = \frac{1}{1 + l'}$$

where l' is the length of the flagella divided by the flagellar length of the DMSO-treated control cells. Inverse length is used so that shorter flagella give a higher score and 1 is added to the denominator to make the maximum shortening factor finite.

Motility Screen. Cells were incubated with drug as above. Plates were scanned on a flatbed scanner at 2 h and at 4 h. Images were imported into Matlab for quantitation of pooling. The green channel was isolated from the composite image, and the image was inverted. Scanning resulted in bright flares reflected on the bottom half of each well. To eliminate this artifact, only the top half of each well was considered. An array of the pixel intensities of the top half of each well was stored and manipulated to determine the variances of each. Wells with strongly pooled cells showed a much higher variance (~900) than wells with homogeneous cell distribution and no pooling (>~100). The within-well standard deviations divided by the standard deviations of control (1% DMSO treated) wells gave the pooling factor, P.

Viability Assay. Cells were treated with drug as above. A 1 μL aliquot was removed from wells and diluted in 99 μL of fresh liquid TAP. Cells were grown without agitation under constant light for 5

917

dx.doi.org/10.1021/cb200349v | ACS Chem. Biol. 2012, 7, 911−919

days. Plates were scanned on a flatbed scanner. Clear wells were scored as cytotoxic.

Hierarchical Clustering. For hierarchical clustering, length measurement was treated as a continuous parameter. Shortening factor was linearly scaled between 0 and 1 to give weight in clustering commensurate with the remaining data sets. Motility assay data was represented by four different binary parameters: the presence/absence of any significant effect on pooling above control levels, presence/absence of slight pooling, intermediate pooling, and strong pooling. These classes were defined by the cutoffs illustrated in Figure 2. Viability was also binary, with 0 representing viable and 1 representing cytotoxic. Likewise the deflagellation parameter was binary, with 1 or 0 indicating the presence or absence of visible severed flagella. The distance matrix was constructed using the Chebychev metric, and the linkage tree was created using average linkage clustering.[42] This combination of metric and clustering algorithm was chosen because they minimized the cophenetic correlation coefficient.[42] As the majority of compounds had no effect at the concentration used for the screens, the inconsistent value cutoff used to generate the final clusters from the dendrogram was selected on the basis of identifying the maximum cluster size that would include ineffective compounds (wild type length, no pooling, not cytotoxic, no deflagellation). This maximum cluster size included 561 compounds. The maximum cluster number preserving the 561-compound cluster was chosen to aid in the identification of pathway-specific clusters.

High Speed Imaging. Live cells pretreated with DMSO as a control or putative paralyzing compound were pipetted onto a glass slide and overlaid with a coverslip with a Vaseline spacer to provide sufficient clearance for swimming. Videos were taken with a Vision Research Miro high speed digital camera at 256×256 resolution and 1000 frames per second. Every 150th frame was used for a montage spanning just over 1 s of real time.

Receptor Expression and Labeling for Cilia Length Measurements in NIH3T3 Cells. We utilized Effectene (Qiagen 301425) to transiently transfect NIH3T3 cells with FLAG tagged Transferrin, Dopamine D1, D2 receptors constructs and examined the cells 3 days post transfection. NIH3T3 cells were fixed with 3.7% formaldehyde and permeabilized with 0.1% Triton X- 100 in PBS, 3% milk and then incubated with DAPI, mouse anti-acetylated tubulin (Sigma F7425, 1 μg/mL for 60 min) and rabbit anti-FLAG antibody (Sigma T6793, 1 μg/mL for 60 min), followed by goat anti-rabbit Alexa594 and goat anti-mouse Alexa488 conjugate (Invitrogen), respectively.

Quantifying Chemical Diversity. Molecules are described using the Extended-Connectivity FingerPrints (ECFP),[43] which encodes their chemical features into a binary fingerprint. This makes comparing chemical structure similarity easy for any given pair of molecules. The Tanimoto coefficient reflects the size of the intersection of the *on* bits (chemical features present in the molecule) in the binary fingerprint over the union. The values of this coefficient range from 0 (no common chemical features) to 1 (reflecting identical compounds), with a value under 0.4 being commonly accepted as a threshold for chemical novelty. All pair-wise Tanimoto coefficients were calculated within each compound set sharing a common phenotype and known target.

ASSOCIATED CONTENT

Ⓢ Supporting Information

This material is available free of charge *via* the Internet at http://pubs.acs.org.

AUTHOR INFORMATION

Corresponding Author
*E-mail: wallace.marshall@ucsf.edu.

Notes
The authors declare no competing financial interest.

ACKNOWLEDGMENTS

REFERENCES

(1) Kozminski, K. G., Johnson, K. A., Forscher, P., and Rosenbaum, J. L. (1993) A motility in the eukaryotic flagellum unrelated to flagellar beating. *Proc. Natl. Acad. Sci. U.S.A. 90*, 5519−5523.

(2) Qin, H., Burnette, D. T., Bae, Y. K., Forscher, P., Barr, M. M., and Rosenbaum, J. L. (2005) Intraflagellar transport is required for the vectorial movement of TRPV channels in the ciliary membrane. *Curr. Biol. 15*, 1695−1699.

(3) Qin, H., Diener, D. R., Geimer, S., Cole, D. G., and Rosenbaum, J. L. (2004) Intraflagellar transport (IFT) cargo: IFT transports flagellar precursors to the tip and turnover products to the cell body. *J. Cell Biol. 164*, 255−266.

(4) Rosenbaum, J. L., and Witman, G. B. (2002) Intraflagellar transport. *Nat. Rev. Mol. Cell Biol. 3*, 813−825.

(5) Silverman, M. A., and Leroux, M. R. (2009) Intraflagellar transport and the generation of dynamic, structurally and functionally diverse cilia. *Trends Cell Biol. 19*, 306−316.

(6) Smith, L. A., Bukanov, N. O., Husson, H., Russo, R. J., Barry, T. C., Taylor, A. L., Beier, D. R., and Ibraghimov-Beskrovnaya, O. (2006) Development of polycystic kidney disease in juvenile cystic kidney mice: insights into pathogenesis, ciliary abnormalities, and common features with human disease. *J. Am. Soc. Nephrol. 17*, 2821−2831.

(7) DiBella, L. M., Park, A., and Sun, Z. (2009) Zebrafish Tsc1 reveals functional interactions between the cilium and the TOR pathway. *Hum. Mol. Genet. 18*, 595−606.

(8) Tammachote, R., Hommerding, C. J., Sinders, R. M., Miller, C. A., Czarnecki, P. G., Leightner, A. C., Salisbury, J. L., Ward, C. J., Torres, V. E., Gattone, V. H. 2nd, and Harris, P. C. (2009) Ciliary and centrosomal defects associated with mutation and depletion of the Meckel syndrome genes MKS1 and MKS3. *Hum. Mol. Genet. 18*, 3311−3323.

(9) Verghese, E., Ricardo, S. D., Weidenfeld, R., Zhuang, J., Hill, P. A., Langham, R. G., and Deane, J. A. (2009) Renal primary cilia lengthen after acute tubular necrosis. *J. Am. Soc. Nephrol. 20*, 2147−2153.

(10) Davis, E. E., Zhang, Q., Liu, Q., Diplas, B. H., Davey, L. M., Hartley, J., Stoetzel, C., Szymanska, K., Ramaswami, G., Logan, C. V., Muzny, D. M., Young, A. C., Wheeler, D. A., Cruz, P., Morgan, M., Lewis, L. R., Cherukuri, P., Maskeri, B., Hansen, N. F., Mullikin, J. C., Blakesley, R. W., Bouffard, G. G., Gyapay, G., Rieger, S., Tonshoff, B., Kern, I., Soliman, N. A., Neuhaus, T. J., Swoboda, K. J., Kayserili, H., Gallagher, T. E., Lewis, R. A., Bergmann, C., Otto, E. A., Saunier, S., Scambler, P. J., Beales, P. L., Gleeson, J. G., Maher, E. R., Attie-Bitach, T., Dollfus, H., Johnson, C. A., Green, E. D., Gibbs, R. A., Hildebrandt, F., Pierce, E. A., and Katsanis, N. (2011) TTC21B contributes both causal and modifying alleles across the ciliopathy spectrum. *Nat. Genet. 43*, 189−196.

(11) Mokrzan, E. M., Lewis, J. S., and Mykytyn, K. (2007) Differences in renal tubule primary cilia length in a mouse model of Bardet-Biedl syndrome. *Nephron Exp. Nephrol. 106*, e88−96.

(12) Murga-Zamalloa, C. A., Atkins, S. J., Peranen, J., Swaroop, A., and Khanna, H. (2010) Interaction of retinitis pigmentosa GTPase regulator (RPGR) with RAB8A GTPase: implications for cilia dysfunction and photoreceptor degeneration. *Hum. Mol. Genet. 19*, 3591−3598.

(13) Walczak-Sztulpa, J., Eggenschwiler, J., Osborn, D., Brown, D. A., Emma, F., Klingenberg, C., Hennekam, R. C., Torre, G., Garshasbi, M., Tzschach, A., Szczepanska, M., Krawczynski, M., Zachwieja, J., Zwolinska, D., Beales, P. L., Ropers, H. H., Latos-Bielenska, A., and Kuss, A. W. (2010) Cranioectodermal dysplasia, Sensenbrenner

syndrome, is a ciliopathy caused by mutations in the IFT122 gene. *Am. J. Hum. Genet.* 86, 949−956.

(14) Kuchka, M. R., and Jarvik, J. W. (1987) Short-flagella mutants of *Chlamydomonas reinhardtii. Genetics* 115, 685−691.

(15) Asleson, C. M., and Lefebvre, P. A. (1998) Genetic analysis of flagellar length control in *Chlamydomonas reinhardtii*: a new long-flagella locus and extragenic suppressor mutations. *Genetics* 148, 693−702.

(16) Barsel, S. E., Wexler, D. E., and Lefebvre, P. A. (1988) Genetic analysis of long-flagella mutants of *Chlamydomonas reinhardtii. Genetics* 118, 637−648.

(17) Berman, S. A., Wilson, N. F., Haas, N. A., and Lefebvre, P. A. (2003) A novel MAP kinase regulates flagellar length in Chlamydomonas. *Curr. Biol.* 13, 1145−1149.

(18) Nguyen, R. L., Tam, L.-W., and Lefebvre, P. A. (2005) The LF1 gene of *Chlamydomonas reinhardtii* encodes a novel protein required for flagellar length control. *Genetics* 169, 1415−1424.

(19) Tam, L.-W., Wilson, N. F., and Lefebvre, P. A. (2007) A CDK-related kinase regulates the length and assembly of flagella in Chlamydomonas. *J. Cell Biol.* 176, 819−829.

(20) Wang, W., and Brautigan, D. L. (2008) Phosphatase inhibitor 2 promotes acetylation of tubulin in the primary cilium of human retinal epithelial cells. *BMC Cell Biol.* 9, 62.

(21) Besschetnova, T. Y., Kolpakova-Hart, E, Guan, Y, Zhou, J, Olsen, B. R., and Shah, J. V. (2009) Identification of signaling pathways regulating primary cilium length and flow-mediated adaptation. *Curr. Biol.* 20, 182−187.

(22) Lefebvre, P. A., Silflow, C. D., Wieben, E. D., and Rosenbaum, J. L. (1980) Increased levels of mRNAs for tubulin and other flagellar proteins after amputation or shortening of Chlamydomonas flagella. *Cell* 20, 469−477.

(23) Dentler, W. L., and Adams, C. (1992) Flagellar microtubule dynamics in Chlamydomonas: cytochalasin D induces periods of microtubule shortening and elongation, and colchicine induces disassembly of the distal, but not proximal, half of the flagellum. *J. Cell Biol.* 117, 1289−1298.

(24) Tuxhorn, J., Daise, T., and Dentler, W. L. (1998) Regulation of flagellar length in Chlamydomonas. *Cell Motil. Cytoskeleton* 40, 133−146.

(25) Engel, B. D., Ishikawa, H., Feldman, J. L., Wilson, C. W., Chuang, P. T., Snedecor, J., Williams, J., Sun, Z., and Marshall, W. F. (2011) A cell-based screen for inhibitors of flagella-driven motility in Chlamydomonas reveals a novel modulator of ciliary length and retrograde actin flow. *Cytoskeleton (Hoboken)* 68, 188−203.

(26) Tuxhorn, J., Daise, T., and Dentler, W. L. (1998) Regulation of flagellar length in Chlamydomonas. *Cell Motil. Cytoskeleton* 40, 133−146.

(27) Nakamura, S., Takino, H., and Kojima, M. K. (1987) Effect of lithium on flagellar length in *Chlamydomonas reinhardtii. Cell Struct. Funct.* 12, 369−374.

(28) Marshall, W. F. (2009) Quantitative high-throughput assays for flagella-based motility in chlamydomonas using plate-well image analysis and transmission correlation spectroscopy. *J. Biomol. Screening* 14, 133−141.

(29) Wilson, N. F., and Lefebvre, P. A. (2004) Regulation of flagellar assembly by glycogen synthase kinase 3 in *Chlamydomonas reinhardtii. Eukaryotic Cell* 3, 1307−1319.

(30) Quarmby, L. M., and Hartzell, H. C. (1994) Two distinct, calcium-mediated, signal transduction pathways can trigger deflagellation in *Chlamydomonas reinhardtii. J. Cell Biol.* 124, 807−815.

(31) Doran, S. A., Koss, R., Tran, C. H., Christopher, K. J., Gallin, W. J., and Goldberg, J. I. (2004) Effect of serotonin on ciliary beating and intracellular calcium concentration in identified populations of embryonic ciliary cells. *J. Exp. Biol.* 207, 1415−1429.

(32) Soliman, S. (1983) Pharmacological control of ciliary activity in the young sea urchin larva. Effects of monoaminergic agents. *Comp. Biochem. Physiol., Part C: Comp. Pharmacol. Toxicol.* 76, 181−191.

(33) Wada, Y., Mogami, Y., and Baba, S. (1997) Modification of ciliary beating in sea urchin larvae induced by neurotransmitters: beat-plane rotation and control of frequency fluctuation. *J. Exp. Biol.* 200, 9−18.

(34) Berbari, N. F., Johnson, A. D., Lewis, J. S., Askwith, C. C., and Mykytyn, K. (2008) Identification of ciliary localization sequences within the third intracellular loop of G protein-coupled receptors. *Mol. Biol. Cell* 19, 1540−1547.

(35) Berbari, N. F., Lewis, J. S., Bishop, G. A., Askwith, C. C., and Mykytyn, K. (2008) Bardet-Biedl syndrome proteins are required for the localization of G protein-coupled receptors to primary cilia. *Proc. Natl. Acad. Sci. U.S.A.* 105, 4242−4246.

(36) Domire, J. S., Green, J. A., Lee, K. G., Johnson, A. D., Askwith, C. C., and Mykytyn, K. (2010) Dopamine receptor 1 localizes to neuronal cilia in a dynamic process that requires the Bardet-Biedl syndrome proteins. *Cell. Mol. Life Sci.* 68, 2951−2960.

(37) Jin, H., White, S. R., Shida, T., Schulz, S., Aguiar, M., Gygi, S. P., Bazan, J. F., and Nachury, M. V. (2010) The conserved Bardet-Biedl syndrome proteins assemble a coat that traffics membrane proteins to cilia. *Cell* 141, 1208−1219.

(38) Marley, A., and von Zastrow, M. (2010) DISC1 regulates primary cilia that display specific dopamine receptors. *PLoS One* 5, e10902.

(39) Ramirez, A. R., Castro, M. A., Angulo, C., Ramio, L., Rivera, M. M., Torres, M., Rigau, T., Rodriguez-Gil, J. E., and Concha, I. I. (2009) The presence and function of dopamine type 2 receptors in boar sperm: a possible role for dopamine in viability, capacitation, and modulation of sperm motility. *Biol. Reprod.* 80, 753−761.

(40) Abdul-Majeed, S., and Nauli, S. M. (2011) Dopamine receptor type 5 in the primary cilia has dual chemo- and mechano-sensory roles. *Hypertension* 58, 325−331.

(41) Nichols, D. E., and Nichols, C. D. (2008) Serotonin receptors. *Chem. Rev.* 108, 1614−1641.

(42) Hastie, T., Tibshirani, R., and Friedman, J. H. (2009) The elements of statistical learning data mining, inference, and prediction, in *Springer Series in Statistics*, 2nd ed., pp xxii, Springer, New York.

(43) Rogers, D., and Hahn, M. (2010) Extended-connectivity fingerprints. *J. Chem. Inf. Model.* 50, 742−754.